Peer-reviewed version available at *Molecules* **2018**, *23*, 1423; doi:10.3390/molecules23061423

Selective interactions with various G-quadruplex DNA forming sequences by berberine and palmatine analogues

Marco Franceschin[1,*], Lorenzo Cianni[1], Massimo Pitorri[1], Emanuela Micheli[2], Stefano Cacchione[2], Claudio Frezza[3,*], Mauro Serafini[3], Minghou Hu[4], Huafi Su[4], Zhishu Huang[4], Lianquan Gu[4], Armandodoriano Bianco[1]

[1] Dipartimento di Chimica, [2] Dipartimento di Biologia e Biotecnologie;
[3] Dipartimento di Biologia Ambientale: Università di Roma "La Sapienza", Piazzale Aldo Moro 5 - 00185, Rome (Italy)
[4] School of Pharmaceutical Sciences, Sun Yat-sen University, Guangzhou, 51010 China

Corresponding authors: Dr. Marco Franceschin, PhD; Dr. Claudio Frezza, PhD
Corresponding authors' e-mail addresses: marco.franceschin@uniroma1.it; claudio.frezza@uniroma1.it
Corresponding authors' telephone number: 0039-0649913622
Corresponding authors' fax number: 0039-0649913841

Abstract

In this article/review, the selective interactions of several berberine and palmatine derivatives with various DNA G-quadruplex structures are reported. These derivatives were constructed starting from two natural compounds, berberine and palamatine, through specific synthetic passages following two different schemes for each of them and using several substituents. The details of these synthesis are also described. Indeed, the study of the interactions of these derivative compounds with various G-quadruplex forming sequences was carried out by means of various structural and biochemical techniques. The results show that the presence of suitable side chains are very useful to improve the interaction of the ligands with G-quadruplex structures. Thus, since G-quadruplex formation is promoted by these compounds, which have never been reported before, these may be tested as potential anticancer drugs.

Keywords: G-quadruplex DNA, interactions, berberine and palmatine analogues, chemotherapy, NMR, FRET and MST assays.

1. Introduction

G-quadruplex is a particular helical tertiary structure of DNA and RNA which is formed by sequences extremely rich in guanine. This structure is the result of the stacking of at least two Guanine tetrad subunits, each of them, formed by the association of four guanines in a square planar geometry which is kept together by the Hoogsteen hydrogen bonds occurring among the bases and further stabilized by a cation, mostly sodium and potassium, in physiological environment [1, 2]. G-quadruplex has been shown to exist widely in the genome and in the transcriptome including human telomeres [3], oncogenic promoters [4-6] and 5'-untranslated region (5'-UTR) of mRNA [7]. Nevertheless, it has been also reported that G-quadruplex can inhibit the activity of telomerase which adds telomeric repeats to the ends of chromosomes and maintains the proliferation of cancer cells [8]. Moreover, it can suppress the expression of specific oncogenes such as *c-kit* which is related to the increasing of cellular proliferation in a variety of different malignant tumors [9, 10]. Thus, tumor cell proliferation can be hampered by small molecules that can facilitate the G-quadruplex formation and/or stabilize its structure.

Among all the existing natural classes of substances, alkaloids are gaining more and more attention for their potential therapeutic purposes due to their high efficacy and low systemic toxicity. In fact, these compounds are well-known to possess strong anticancer, antiasthma, antiviral, antiarrhythmic, analgesic, antibacterial, antihyperglycemic and antimalarial activities [11-15].

Within the alkaloid class, berberine and palmatine (Figure 1) represent two major compounds which have been proved to inhibit telomere elongation and to stabilize G-quadruplex, respectively [16, 17]. Moreover, both of them are natural compounds, having been abundantly isolated from plant sources and, in particular, berberine from *Berberis vulgaris* L. [18] and palamatine from *Coptis japonica* (Thunb.) Makino [19]. From the chemical standpoint, they are quaternary ammonium salts but berberine belongs to the sub-class of benzyl-isoquinoline alkaloids whereas palmatine is a simple isoquinoline alkaloid.

Peer-reviewed version available at *Molecules* **2018**, *23*, 1423; doi:10.3390/molecules23061423

Figure 1 near here

Previous interaction studies of these compounds with DNA have clearly revealed a midlle interaction between them all by a mechanism of intercalation [20, 21]. Yet, the same studies have also indicated their low selectivity and low thermodynamic stability with G-quadruplex [20, 21].

For these reasons, several efforts have been undertaken to improve their ability to stabilize G-quadruplex [22-25].

Our research group has also focused its attention on this matter. Yet we adopted a strategy based on using short oligonucleotides to help the bond to the complementary DNA bases that become accessible after the formation of G-quadruplex. In fact, it has been widely reported that the combination of selected peptides to DNA binding scaffolds would greatly increase their selectivity to G-quadruplex versus duplex DNA. For example, this has been observed for human cathelicidin peptide LL37 that was at least 10 times more selective to G-quadruplex structures in comparison to duplex DNA [26]. On this basis, a series of berberine and palmatine derivatives have been developed, characterized by the presence of further side chains on the base structures of these compounds [23, 27].

In this review, the design, the chemical synthesis and the NMR and MS identification data of different derivatives of berberine and palmatine developed in our laboratory are reported. These derivatives have never been described before as well as the primary efficacy evaluation of them as DNA G-quadruplex stabilizers. Several side chains have been taken into consideration and a comparison among the different results has also been performed. The final aim of this review was to provide a general overview on the possible ways of action in synthesizing alkaloid compounds with potential antitumoral activity by interaction with DNA G-quadruplex, starting from natural phytochemicals.

2. Results and Discussion

2.1. Synthesis of berberine and palmatine derivatives

The synthetic pathway followed for the design of the berberine derivatives is reported in Scheme 1, while the synthetic pathway followed for the design of the 9-peptidyl-palmatine derivatives is reported in Scheme 2.

Scheme 1 near here

Scheme 2 near here

The two schemes fully show that two different pathways were taken into consideration to build the possible ligands of G-quadruplex starting from berberine and palmatine. In particular, one only berberine derivative with only one organic side chain was developed whereas several palmatine derivatives with different side chains were realized (Scheme 3).

Scheme 3 near here

This different choice is due to an extensive observation of literature data that mainly refer to palmatine. In fact, a couple of studies have previously demonstrated two important things: the first one is that palmatine derivative compounds with side chains having terminal amino groups are more able to stabilize G-quadruplex DNA which significantly improves their inhibitory activity on telomerase [28]; the second one is that the specific presence of amino acid chains on quinolidine structures deeply increases the ability of these compounds to interact with the G-quadruplex [28]. The latter factor seems to have nothing to do with the research but it is actually the opposite. In fact, the ring system of palmatine resembles much that of quindoline and it might be expected that similar situations may lead to similar results. So, on the basis of such assumption, several palmatine derivatives with peptide side chains were prepared also in order to evaluate their single eventual contributions on the total effect .

On the other hand, only a few possible derivatives of berberine have been synthesized and tested till now with a piperidin side chain [29-30] but this has never been done in association with berberine.

2.2. Interaction studies of the compounds with G-quadruplex

The figure below (Figure 2) reports on the ability of the derivative compound of berberine (**4**) to induce the formation of inter- and intramolecular G-quadruplex structures.

Figure 2 near here

This ability was investigated by polyacrylamide gel electrophoresis (PAGE) using the DNA oligonucleotides 2HTR and TSG4 as models. 2HTR is constituted by this sequence (5'-AATCCGTCGAGCAGAGTTAGGGTTAGGGTTAG-3') and is known, by literature [31], to form only dimeric and/or tetrameric intermolecular G-quadruplex structures whereas TSG4 with this sequence (5'-GGGATTGGGATTGGGATTGGGTT-3'), is known to form also intramolecular G-quadruplex structures [30].

The analysis was performed at different drug concentrations, 10 μM (lane 1), 30 μM (lane 2), 50 μM (lane 3), 70 μM (lane 4) and 100 μM (lane 5) and evidenced that compound (**4**) is able to induce G-quadruplex dimeric structures on 2HTR but not on TSG4.

On the other hand, the ability of compounds (**9a-9g**) to bind and stabilize G- quadruplex structures was evaluated by several studies.

In order to study the influence of the peptide side chains on palmatine scaffold, molecular docking was performed on four different parallel G-quadruplex structures formed by sequences thoroughly studied in literature i.e. Bcl2, c-Kit, c-Myc which are comprised in some oncogene promoters and hTG21 which ontains human telomeric G-rich repeats.

The results are reported in Table 1 and show that, in general, compounds (**9a-9g**) possess a higher affinity of bond with G- quadruplex structures than palmatine. However compounds (**9a-9g**) show a flat SAR on the different DNA strands and this effect could be explained by a limitation of the technique itself.

Table 1 near here

Yet, it's important to underline the fact that these values are indicative on a relative scale for studying the behavior of similar compounds [32].

Nevertheless our results show a good accordance with the model already present in literature [33]. Indeed, the core of the ligand (**9a**) interacts with the aromatic area of the G-tetrad while the side chain (RR) is inserted in the groove of the DNA as showed in figure 3.

Figure 3 near here

All the synthesized compounds were also evaluated for their thermodynamic stability and selectivity to G-quadruplex over duplex DNA through Fluorescence Resonance Energy

Transfer (FRET) Melting assay. The G-quadruplex sequences used in this assay were Fc-*kit*1T, FPu18T and again F21T. Fc-*kit*1T is an oligonucleotide constituted by the sequence 5'-FAM-d[AGGGAGGGCGCTGGGAGGAGGG]-TAMRA-3' and represents the c-*kit* promoter DNA sequence whereas FPu18T is an oligonucleotide constituted by the sequence 5'-FAM-d[AGGGTGGGGAGGGTGGGG]-TAMRA-3' and represents the oncogene c-myc promoter DNA sequence. The F10T sequence (5′-FAM-d[TATAGCTATA-HEG-TATAGCTATA]-TAMRA-3') was used as non-quadruplex control because it is a self-complementary duplex DNA hairpin [34].

In a previous study of this kind with berberine and its derivative [23] using F21T, it was evidenced that compound (**4**) has a major effect on the G-quadruplex stability than berberine alone. Indeed, compound (**4**) was seen to have no significant effect on the melting temperature of DNA with a $\Delta T_m < 1$ °C, after FRET melting assay experiments with F21T that is constituted by the sequence 5'-FAM-dGGGTTAGGGTTAGGGTTAGGG-TAMRA-3'. This last analysis is useful to determine the ligand-induced stabilization of a folded quadruplex by measurement of the ligand induced increasing in the melting temperature (ΔT_m) [35].

On the other hand, Figure 4 and Table 2 below show the results for palmatine and its derivatives (**9a-9g**).

Figure 4 near here

Table 2 near here

These reveal that the ligands can increase the stabilization of the G-quadruplex sequence with a wide range of ΔT_m values. The stabilizing activities of the tested compounds toward c-*kit* G-quadruplex (ΔT_m value of 6.1-21.7 °C) and c-*myc* G- quadruplex (ΔT_m value of 5.0-23.8 °C) in promoter were found to be better than telomeric G-quadruplex (ΔT_m value of 0.0-11.0 °C). Comparing ligands with different peptidyl length, the results showed that ligands **9a**, **9b**, **4g** with dipeptidyl side chain were better than other ligands **9d**, **9e**, **9f**, **9g** with a longer chain length.

From these data, it was possible to establish that side chains with more than two amino acids on palmatine derivatives reduce the ability of the compound to stabilize the G-quadruplex structure. Probably this depends to the size of the loop and the ability to

accommodate a peptide basic side chain. However we have an important gain in selectivity G-quadruplex on Duplex for most of the synthesized compounds.

According to these results, the Microscale Thermophoresis (MST) assay was used to further investigate the binding affinity of ligands for *c-kit* quadruplex and their level of specificity for *c-kit* quadruplex versus duplex DNA. This technique is a highly sensitive probe for many kinds of binding-induced interactions such as molecular size, charge, hydration shell or conformation [36] and possesses several advantages including easy implementation, faster speed (about 1 min), lower sample requirements (e.g., microliter volumes), no limitations on molecular size or weight fro the binding partners and the possibility of usimg several buffer solutions [37].

Tables 3 and 4 and Figures 5, 6 and 7 show the results of this analysis.

Table 3 near here

Figure 5 near here

Table 4 near here

Figure 6 near here

Figure 7 near here

As shown, all tested ligands were found to bind to the *c-kit* G-quadruplex more tightly than to duplex DNA (*c-kit* G-quadruplex K_d, 1.41-11.1 μM; duplex K_d, 10.7-45.5 μM). From these data, it could be clearly sees that the introduction of peptidyl side chain onto the scaffold of palmatine gives a moderate improvement of its specificity for quadruplex over duplex DNA compared with palmatine ($K_d^{duplex}/K_d^{c\text{-}kit1}$ = 1.6). The ligands **9a**, **9b**, **9c** ($K_d^{duplex}/K_d^{c\text{-}kit1}$ value ranging from 7.6 to 13.9) with dipeptidyl side chain had more binding affinity and selectivity to *c-kit* G-quadruplex DNA than ligands **9d**, **9e**, **9f**, **9g** ($K_d^{duplex}/K_d^{c\text{-}kit1}$ value ranging from 2.1 to 4.2) with a longer chain length. All these results were approximately consistent with their ΔT_m values obtained from FRET melting assays.

4. Materials and Methods

4.1. Materials

Pure berberine and palmatine were purchased from Sigma-Aldrich as well as the other natural solvents of RPE purity grade, if not diversely specified, and the deuterated solvents.

The Fmoc protected amino acids and Rink amide AM resin were purchased from GL Biochem (Shanghai) Ltd..

All oligomers/primers were purchased from Invitrogen and Sangon Biotech (China).

Stock solutions of all the derivatives (10 mM) were made using DMSO (10%) or double-distilled deionized water.

Silica gel for classical Column Chromatography (40-63 μm particle size) was purchased from Fluka Analytical while silica gel for Flash Column Chromatography (200-300 mesh) was purchased from Qingdao Haiyang Chemical Co. Ltd.

4.2. Instrumentation

^{1}H-NMR and ^{13}C-NMR spectra were recorded on a Varian (now Agilent Technologies) Mercury 300 MHz spectrometer and/or on a Bruker BioSpin GmbH 400 MHz spectrometer using $CDCl_3$, CD_3OD, D_2O and DMSO as deuterated solvents. The chemical shifts were expressed from TMS (s, 0 ppm) for spectra in $CDCl_3$, the internal solvent signal of CD_2HOD (m5, 3.31 ppm) was the reference for spectra in CD_3OD, the HDO signal (s, 4.79 ppm) was set as reference for spectra in D_2O whereas the internal solvent signal of D_3SOD_3 (p, 2.50 ppm) was the reference for spectra in DMSO-d_6.

Mass spectra were recorded on a Shimadzu LCMS-2010A instrument or on a Q-TOF MICRO spectrometer (Micromass, now Waters, Manchester, UK) instrument. The first instrument had an ESI-API ion source whereas the second instrument had only an ESI ion source. Both instrument operated in positive ionization with a voltage of 5000 V. The flow rates of sample infusion for both instruments were 30 μL/min. with 50 acquisitions per spectrum. Data coming from both instruments were analyzed by using the MassLynx software developed by Waters.

High resolution mass spectra (HRMS) were performed on a Shimadzu LCMS-IT-TOF instrument with the same characteristics as previously described.

The purification of the reaction mixtures was achieved by means of classical Column Chromatography on silica gel, by means of Flash Column Chromatography or by means of Inverse Column Chromatography with stationary phase (C18)-bonded silica (USP classification L1) whereas the purification of all the tested compounds was processed with preparative HPLC using a Varian Pro Star equipped with an UV-vis detector (BioRad) and a Phenomenex C18 (10.0 × 250 mm, 5 µm) column.

The microwave reaction was performed with Biotage Initiatior.

The radioactivity was quantified by using a Beckman LS 5000 TD Scintillation System.

Complexes and structures formed after incubation were studied by native PAGE (15% polyacrylamide gel, TBE 0.5·, KCl 20 mM, run overnight at 4 °C)

DNA melting curves were obtained by 260 nm absorbance measurement on a UV-Vis spectrophotometer (JASCO V-530). The temperature range was covered in 70 min, and the absorbance values were collected every 10 s.

Other instruments are specified further on.

4.3. Synthesis

4.3.1. Berberine derivatives

4.3.1.1. Synthesis of compound (4)

3.0 g of berberine chloride (8.07 mmol) were dissolved in 18 ml of water and then 4.5 ml of NaOH 50% solution was added. While stirring, 3.0 ml of acetone was added dropwise. After stirring for 30 min at room temperature, the reaction mixture was filtered and washed with 80% methanol to give 2.65 g of the final product with a yield of 83.5%.

This was used for the next reaction without any further purification and was dissolved in 75 ml of CH_3CN. Then 7.4 ml of 1,3-diiodopropane were added and the solution was stirred at 80 °C for 6 h. After cooling, the product was filtered, washed repeatedly with acetonitrile and purified by column chromatography on silica gel ($CHCl_3$–MeOH in ratio 9:1 (v/v) and then 8:2 (v/v)) to give 370 mg of the final product with a yield of 8.7%.

This was directly put under reaction with 0.86 ml of piperidine in 36 ml of refluxing ethanol for 4 h. After cooling, the reaction mixture was dried under vacuum and the crude product

was purified by silica gel column chromatography equilibrated with 10% of water ($CHCl_3$) to give 265 mg of the final product with a yield of 77%.

Compound (**4**) was obtained by dissolving compound (**3**) in 0.1 MHCl and after passing it through a Dowex1 strong basic anion exchange resin. The acid solution was concentrated under vacuum, adding repeatedly an equal volume of chloroform, until a powder was formed corresponding to the final product.

4.3.1.2. Synthesis of labeled oligomers

The DNA oligomers 2HTR and TSG4 were 50-end labeled by T4 polynucleotide kinase (2.5 U/lg DNA) for 30 min at 37 °C in 50 µL buffer containing 50 mM Tris–HCl, pH 7.5, 10 mM $MgCl_2$, 10 mM 2-mercaptoethanol and 30 µCi [c-32P] ATP. The reaction was quenched by heating the mixture at 65 °C for 10 min. The reaction mixture was then purified through phenol/chloroform and chloroform extractions. After precipitation with ammonium acetate and ethanol and washing with 80% ethanol, the DNA was dried and then dissolved in water. Radioactivity was quantified.

4.3.1.3. Preparation of the DNA

1 mg/ml solution of calf thymus DNA was sonicated to about 500 bp fragments. Sonicated DNA and drug stocks were mixed to obtain a 1 ml solution containing 30 µM DNA, 50 mM potassium cacodylate (pH 7.4) and 3 or 30 µM drugs for [drugs]/[DNA] in ratio 0.1 (v/v) and 1 (v/v), respectively.

4.3.1.4. Adding of the drugs

Drugs were added at different concentrations to the reaction mixture (50 lL), containing 50 lM dNTPs, 0.5 µM TSG4 primer and 1 µL of cell extract (prepared from 10^9 cultured HeLa cells as previously described) in TRAP buffer (20 mM Tris–HCl (pH 7.5), 68 mM KCl, 15 mM MgCl2, 10 mM EDTA and 0.5% Tween 20). Samples were incubated for 2 h at 30 °C, before the addition of the cell extract. After 30 min of incubation at 30 °C, the samples were purified by phenol/chloroform extraction. 32P radiolabelled TSG4, 0.5 lM CXext and 2 U Taq DNA polymerase (Eppendorf) were added and 27 PCR cycles were performed (94 °C 30", 50 °C 30" and 72 °C 1'3O"). Finally, the samples were loaded on nondenaturing 12%

polyacrylamide gel. Samples with no drug and with no cell extract were references. A 130 bp "internal standard2 (IS) was used to evaluate PCR amplification efficiency [38].

4.3.2. For palmatine derivatives

The synthesis of the derivative compounds of palmatine (compounds **6**, **7**, **8**) was achieved by using a similar procedure as reported in literature for berberine [22] but modified by us. In particular, the first step was optimized for the microwave reaction by increasing the quantity of reagent and keeping a high yield while the purification was performed on an inverse chromatographic column by using a mixture of CH_3OH/H_2O with 1% of TFA from 5:95 (v/v) to 1:1 (v/v).

To have compound (**6**), the reaction was performed under microwave irradiation. A quantity of palmatine for the weight of 2 g (5.15 mmol) was added in a flask provided with a stir bar. The solution was pre-stirred for 1 min before raising the temperature. The machine was programmed to high levels of absorption. The solution was heated to 180°C, with a voltage of 400W, for 5-10 minutes. The reaction gave a red precipitate (compound (**2**)) that was washed and filtered with ether under vacuum with a final yield of 95%.

Compound (**6**) present in CH_2Cl_2, was treated with the ethyl ester of bromoacetic acid in ratio 1:2 (v/v), stirred on a magnetic stirrer, and refluxed for 12 h as suggested in literature [39]. The resulting yellow precipitate was filtered off, refluxed with EtOH for 30 min, cooled, filtered off again and dried in vacuum to give the final compound with a yield of 55%.

Compound (**7**) was dissolved in a solution of CH_3OH/H_2O (1:1 (v/v)). Then, NaOH in ratio 1:2 (w/w), was added under reflux for 12 h on a water bath and the solution was cooled [39]. At this point, HCl was added until a pH value of 1. The resulting yellow precipitate was filtered off and dried in vacuo to give the final compound with a yield of 45 %.

To have compounds (**9a-9g**), the intermediate compound (**8**) for the weight of 200 mg was mixed with deprotected peptidyl side chains using DIC/HOBT (475 mg/500 mg) in DMF (4 mL) with shaking for 12 h. After coupling with compound (**8**), the resin was treated with the cleavage reagent (95% TFA, 5% dd H_2O (v/v)) for 2 h, washed with dry ether (30 mL), and then evaporated under vacuum. The crude products were purified by using preparative RP-HPLC with CH_3CN/H_2O (95:5 to 5:95) containing 0.1% TFA at a flow rate of 2.5 mL/min elution, and then lyophilized to give the final compounds,

Peptidyl side chains were synthesized using solid-phase methodology by manual operation of a peptide synthesizer. The Fmoc protected various amino acids (4 equiv ratio excess to the

resin) were coupled orderly to the Rink amide AM resin (500 mg) using DIC/HOBT (190 mg/200 mg) in DMF (4 mL) for 3 h. The deprotection of the Fmoc group was carried out with piperidine/DMF 25% (2 mL) for 30 min.

For compound (**9a**), the peptidyl coupling order is Arginine-Lysine and this was a yellow solid with a yield of 10%.

For compound (**9b**), the peptidyl coupling order is Arginine-Phenylalanine and this was a yellow solid. The yield was 29%.

For compound (**9c**), the peptidyl coupling order is Arginine-Arginine and this was a yellow solid. The yield was 5%.

For compound (**9d**), the peptidyl coupling order is Arginine-Histidine-Glycine and this was a yellow solid. The yield was 5%.

For compound (**9e**), the peptidyl coupling order is Arginine-Lysine-Phenylalanine and this was a yellow solid. The yield was 10%.

For compound (**9f**), the peptidyl coupling order is Lysine-Glycine-Arginine and this was a yellow solid. The yield was 8%.

For compound (**9g**), the peptidyl coupling order is Arginine-Lysine- Phenylalanine and this was a yellow solid. The yield was 10%.

4.4. NMR and MS data of all the synthetic compounds

4.4.1. Berberine derivatives

8-acetonyl-dihydroberberine (**1**): NMR and MS data are reported in the work by Franceschin et al., 2006 [23].

13-(3-Iodopropyl)berberine iodide (**2**): NMR and MS data are reported in the work by Franceschin et al., 2006 [23].

13-[3-(1-Piperidino)propyl]berberine iodide (**3**): NMR and MS data are reported in the work by Franceschin et al., 2006 [23].

13-[3-(1-Piperidino)propyl]berberine hydrochloride (piperidino-berberine): NMR and MS data are reported in the work by Franceschin et al., 2006 [23].

4.4.2. Palmatine derivatives

3-hydroxy-2,16,17-trimethoxy-11,12-dihydroisoquinolino[9,8-a]isoquinolin-7-ium chloride (**6**) (Figure 8): ^{1}H-NMR (400 MHz, DMSO) δ: 9.11 (1H, s, H-7), 8.08 (1H, s, H-10), 7.52 (1H, s, H-18), 7.24 (2H, t, *J* = 6.4 Hz, H-6), 6.99 (1H, s, H-15), 6.40 (2H, d, *J* = 6.4 Hz, H-1), 4.50 (2H, t, *J* = 4.4 Hz, H-11), 3.90 (3H, s, OCH_3-17), 3.83 (3H, s, OCH_3-16), 3.74 (3H, s, OCH_3-2), 3.07 (2H, t, *J* = 4.4Hz, H-12).
ESI-API-MS: *m/z* 338.1 $[M]^+$ (calculated for $C_{20}H_{20}NO_4$, 338.4 $[M]^+$)

3-(2-ethoxy-2-oxoethoxy)-2,16,17-trimethoxy-11,12-dihydroisoquinolino[9,8-a]isoquinolin-7-ium (**7**) (Figure 8): ^{1}H-NMR (400 MHz, DMSO) δ: 9.93 (1H, s, H-7), 9.02 (1H, s, H-10), 8.20 (2H, d, *J* = 8.2 Hz, H-6), 8.02 (2H, d, *J* = 8.2 Hz, H-1), 7.71 (1H, s, H-18), 7.10 (1H, s, H-15), 5.06 (2H, s, H-19), 4.94 (2H, t, *J* = 4.9 Hz, H-11), 4.17 (2H, q, *J* = 4.1 Hz, H-22), 4.03 (3H, s, OCH_3-17), 3.93 (1H, s, OCH_3-16), 3.87 (1H, s, OCH_3-2), 3.22 (2H, t, *J* = 4.9 Hz, H-12), 1.19 (3H, t, *J* = 4.1 Hz, H-23).
ESI-API-MS: *m/z* 424.3 $[M]^+$ (calculated for $C_{24}H_{27}NO_6$, 424.5 $[M]^+$)

3-(carboxymethoxy)-2,16,17-trimethoxy-11,12-dihydroisoquinolino[9,8-a]isoquinolin-7-ium (**8**) (Figure 8): ^{1}H-NMR: (400 MHz, DMSO) δ: 10.4 (1H, s, H-7), 8.98 (1H, s, H-10), 7.59 (2H, d, *J* = 8.2 Hz, H-6), 7.49 (2H, d, *J* = 8.2 Hz, H-1), 7.43 (1H, s, H-18), 6.94 (1H, s, H-15), 4.26 (2H, s, H-19), 4.15 (2H, t, *J* = 4.9 Hz, H-11), 3.88 (3H, s, OCH_3-17), 3.87 (3H, s, OCH_3-16), 3.82 (1H, s, OCH_3-2), 3.22 (2H, t, *J* = 4.9 Hz, H-12).
ESI-API-MS: *m/z* 396.1 $[M]^+$ (calculated for $C_{22}H_{23}NO_6$, 396.4 $[M]^+$)

Figure 8 near here

3-(2-(((*S*)-6-amino-1-(((*S*)-1-amino-5-guanidino-1-oxopentan-2-yl)amino)-1-oxohexan-2-yl)amino)-2-oxoethoxy)-2,16,17-trimethoxy-11,12-dihydroisoquinolino[9,8-a]isoquinolin-7-ium (**9a**) (Figure 9): ^{1}H-NMR (400MHz, CD_3OD) δ: 9.95 (1H, s, H-7), 8.83 (1H, s, H-10), 8.16 (1H, d, *J* = 8.0 Hz, H-6), 8.14 (1H, d, *J* = 8.0 Hz, H-1), 7.68 (1H, s, H-18), 7.06 (1H, s, H-15), 6.09 (2H, t, *J* = 6.0 Hz, H-11), 4.95 (2H, s, H-11), 4.39 (1H, m, H-22), 4.26 (1H, m, H-29), 4.13 (3H, s, OCH_3-17), 4.07 (2H, m, H-34), 4.00 (3H, s, OCH_3-16), 3.95 (3H, s, OCH_3-

2), 3.22 (2H, t, *J* = 6.0 Hz, H-12), 3.20 (2H, m, H-26), 1.71 (10H, m, H-23, H-24, H-25, H-32, H-33).
HR-MS (LC-MS-IT-TOF): *m/z* 580.6512 $[M]^+$.

9-(3-(((*S*)-1-(((*S*)-1-amino-6-guanidino-1-oxohexan-2-yl)amino)-1-oxo-3-phenylpropan-2-yl)amino)-3-oxopropyl)-2,16,17-trimethoxy-11,12-dihydroisoquinolino[9,8-a]isoquinolin-7-ium (**9b**) (Figure 9): ^{1}H-NMR (400MHz, CD_3OD) δ: 9.96 (1H, s, H-7), 8.72 (1H, s, H-10), 8.14 (1H, d, *J* = 8.0 Hz, H-6), 8.05 (1H, d, *J* = 8.0 Hz, H-1), 7.66 (1H, s, H-18), 7.15 (5H, m, H-25, H-26, H-27, H-28, H-29), 7.05 (1H, s, H-15), 6.11 (2H, t, *J* = 6.0 Hz, H-11), 4.95 (2H, s, H-19), 4.47 (1H, m, H-31), 4.13 (3H, s, OCH_3-17), 4.12 (3H, s, OCH_3-16), 4.09 (3H, s, OCH_3-2), 4.07 (2H, m, H-35), 3.16 (2H, d, *J* = 6.0 Hz, H-12), 1.71 (4H, m, H-23, H-33).
HR-MS (LC-MS-IT-TOF): *m/z* 698.3296 $[M]^+$.

3-(2-(((*S*)-5-((1-aminovinyl)amino)-1-oxo-1-(((*S*)-2-oxo-6-(prop-1-en-2-ylamino)hexan-3-yl)amino)pentan-2-yl)amino)-2-oxoethoxy)-2,16,17-trimethoxy-11,12-dihydroisoquinolino [9,8-a]isoquinolin-7-ium (**9c**) (Figure 9): ^{1}H-NMR (400MHz, CD_3OD) δ: 9.96 (1H, s, H-7), 8.72 (1H, s, H-10), 8.14 (1H, d, *J* = 8.0 Hz, H-6), 8.05 (1H, d, *J* = 8.0 Hz, H-1), 7.66 (1H, s, H-18), 7.05 (1H, s, H-15), 6.04 (2H, t, *J* = 6.0 Hz, H-11), 4.95 (2H, s, H-19), 4.69 (1H, m, H-30), 4.47 (1H, m, H-22), 4.13 (3H, s, OCH_3-17), 4.12 (3H, s, OCH_3-16), 4.09 (3H, s, OCH_3-2), 4.07 (4H, m, H-26, H-34), 3.16 (2H, d, *J* = 6.0 Hz, H-12), 1.87 (4H, m, H-23, H-32), 1.71 (8H, m, H-24, H-25, H-32, H-33).
HR-MS (LC-MS-IT-TOF): *m/z* 707.3623 $[M]^+$.

5-guanidino-2-[[3-(1H-imidazol-4-yl)-2-[[3-phenyl-2-[[2-[(2,16,17-trimethoxy-11,12-dihydroisoquinolino[9,8-a]isoquinolin-7-ium-9-yl)oxy]acetyl]amino]propanoyl]amino] propanoyl]amino]pentanamide (**9d**) (Figure 9): ^{1}H-NMR: (400MHz, CD_3OD) δ: 9.89 (1H, s, H-7), 8.78 (1H, s, H-10), 8.16 (1H, d, *J* = 8.0 Hz, H-6), 8.10 (1H, d, *J* = 8.0 Hz, H-1), 7.99 (1H, s, H-36), 7.70 (1H, s, H-18), 7.20 (5H, m, H-25, H-26, H-27, H-28, H-29), 7.08 (1H, s, H-15), 7.05 (1H, s, H-35), 6.08 (2H, t, *J* = 6.0 Hz, H-11), 4.95 (2H, s, H-19), 4.71 (1H, m, H-30), 4.54 (1H, m, H-22), 4.36 (1H, m, H-38), 3.97 (3H, s, OCH_3-17), 3.93 (3H, s, OCH_3-16), 3.88 (3H, s, OCH_3-17), 3.91 (2H, s, H-34), 3.79 (2H, m, H-19), 3.20 (2H, m, H-42), 3.18 (2H, t, *J* = 6.0 Hz, H-12), 1.90 (2H, m, H-41), 1.71 (2H, m, H-40).
HR-MS (LC-MS-IT-TOF): *m/z* 835.9367 $[M]^+$.

6-amino-*N*-[1-benzyl-2-[(1-carbamoyl-4-guanidino-butyl)amino]-2-oxo-ethyl]-2-[[2-[(2,16,17-trimethoxy-11,12-dihydroisoquinolino[9,8-a]isoquinolin-7-ium-9-yl)oxy]acetyl]amino] hexanamide (**9e**) (Figure 9): ^{1}H-NMR (400MHz, CD_3OD) δ: 9.96 (1H, s, H-7), 8.73 (1H, s, H-10), 8.13 (1H, d, *J* = 8.0 Hz, H-6), 8.05 (1H, d, *J* = 8.0 Hz, H-1), 7.50 (1H, s, H-18), 7.22 (5H, m, H-34, H-35, H-36, H-37, H-38), 7.12 (1H, s, H-15), 6.05 (2H, t, *J* = 6.0 Hz, H-11), 4.96 (2H, s, H-19), 4.81 (1H, m, H-29), 4.74 (1H, m, H-22), 4.66 (1H, m, H-39), 4.02 (3H, s, OCH_3-17), 4.01 (3H, s, OCH_3-16), 3.98 (3H, s, OCH_3-2), 3.81 (2H, m, H-43), 3.21 (2H, m, H-32), 3.20 (2H, m, H-26), 3.03 (2H, t, *J* = 6.0 Hz, H-12), 1.90 (4H, m, H-42), 1.71 (2H, m, H-24, H-41), 1.65 (2H, m, H-25).
HR-MS (LC-MS-IT-TOF): *m/z* 858.4319 $[M]^+$.

6-amino-2-[[2-[[3-phenyl-2-[[2-[(2,16,17-trimethoxy-11,12-dihydroisoquinolino[9,8-a]isoquinolin-7-ium-9-yl)oxy]acetyl]amino]propanoyl]amino]acetyl]amino]hexanamide (**9f**) (Figure 9): ^{1}H-NMR (400MHz, CD_3OD) δ: 9.94 (1H, s, H-7), 8.74 (1H, s, H-10), 8.13 (1H, d, *J* = 8.0 Hz, H-6), 8.06 (1H, d, *J* = 8.0 Hz, H-1), 7.75 (1H, s, H-18), 7.23 (5H, m, H-25, H-26, H-27, H-28, H-29), 7.12 (1H, s, H-15), 6.08 (2H, t, *J* = 6.0 Hz, H-11), 4.92 (2H, s, H-19), 4.70 (1H, m, H-31), 4.41 (1H, m, H-22), 4.09 (2H, s, H-29), 3.99 (3H, s, OCH_3-17), 3.97 (3H, s, OCH_3-16), 3.94 (3H, s, OCH_3-2), 3.61 (2H, m, H-36), 3.13 (2H, t, *J* = 6.0 Hz, H-12), 3.08 (2H, m, H-23), 1.92 (2H, m, H-34), 1.70 (2H, m, H-33), 1.45 (2H, m , H-35).
HR-MS (LC-MS-IT-TOF): *m/z* 727.8355 $[M]^+$.

6-amino-*N*-(1-carbamoyl-4-guanidino-butyl)-2-[[3-phenyl-2-[[2-[(2,16,17-trimethoxy-11,12-dihydroisoquinolino[9,8-a]isoquinolin-7-ium-9-yl)oxy]acetyl]amino]propanoyl] amino]hexanamide (**9g**) (Figure 9): ^{1}H-NMR (400MHz, CD_3OD) δ: 9.98 (1H, s, H-7), 8.69 (1H, s, H-10), 8.15 (1H, d, *J* = 8.0 Hz, H-6), 8.04 (1H, d, *J* = 8.0 Hz, H-1), 7.51 (1H, s, H-18), 7.27 (5H, m, H-25, H-26, H-27, H-28, H-29), 7.12 (1H, s, H-15), 6.02 (2H, t, *J* = 6.0 Hz, H-11), 4.94 (2H, s, H-19), 4.80 (1H, m, H-22), 4.73 (1H, m, H-29), 4.69 (1H, m, H-35), 4.05 (3H, s, OCH_3-17), 4.06 (3H, s, OCH_3-16), 3.95 (3H, s, OCH_3-2), 3.71 (2H, m, H-38), 3.21 (2H, m, H-23), 3.20 (2H, m, H-33), 3.02 (2H, t, *J* = 6.0 Hz, H-12), 1.90 (4H, m, H-32, H-37), 1.70 (4H, m, H-31, H-36), 1.65 (2H, m, H-30).
HR-MS (LC-MS-IT-TOF): *m/z* 858.4319 $[M]^+$.

Figure 9 near here

4.5. Structural and biological analysis

4.5.1. Incubation for PAGE analysis

Oligonucleotides (8 or 12 μM) were heated at 95 °C for 10 min and quickly cooled in ice to disrupt any preformed structures. They were then incubated for 2 h at 30 °C in the presence of different drug concentrations, in MES–KCl buffer (10 mM MES, pH 6.5, 50 mM KCl). In the case of TSG4 a lower KCl concentration was used ([KCl] = 5 mM), because at higher K^+ concentrations, the G-quadruplex monomeric structure is also formed in the absence of drugs. Complexes and structures formed after incubation were studied by native PAGE (15% polyacrylamide gel, TBE 0.5·, KCl 20 mM, run overnight at 4 °C)

4.5.2. Molecular docking

The crystal structure of G-quadruplex DNA was extracted from the Protein Data Bank (PDB; PDB) reported in Table 5.

Table 5 near here

The structures were treated with the Maestro module of Schrödinger Suite 2012 as follows. All sulfate ions and water molecules found in the structure were removed, hydrogen atoms were added, and the H-bond assignment was optimized with exhaustive sampling. Ligand structures were constructed and optimized by using the Maestro 9.3 followed by rebuilding the 3D conformation of each molecule using LigPrep 2.3 at pH of 7.0. Afterwards, the rebuilt ligands were subjected to a conformational search using Macromodel 9.7 with OPLS 2005 force field in a water solvent model. For each DNA, first a grid box of 36 × 36 × 36 Å with a default inner box (10 × 10 × 10 Å) was centered on the DNA itself. For all experiments the standard precision mode of GlideScore was selected as scoring function. The top 10 poses were kept and XP score functions between the ligands and the DNA were analyzed.

4.5.3. FRET Assays

FRET assay was carried out on a real-time PCR apparatus following previously published procedures [40].

The fluorescently labeled oligonucleotides F21T, Fc-*kit*1T, FPu18T and F10T were used as the FRET probes. Fluorescence melting curves were determined with a Roche LightCycler 2 real-time PCR apparatus, using a total reaction volume of 20 μL, with 0.2 μM labeled oligonucleotide in Tris-HCl buffer (10 mM, pH 7.4) containing 60 mM KCl in the presence or absence of 2 μM compounds. Fluorescence readings with excitation at 470 nm and detection at 530 nm were taken at intervals of 1 °C over the range 37-99 °C, with a constant temperature being maintained for 30 s prior to each reading to ensure a stable value. Final analysis of the data was carried out using Origin 8.0 (Origin Lab Corp.).

4.5.3. MST Assays

The fluorescently labeled oligonucleotides (FAM-c-*kit*1, AGGGAGGGCGCTGGG-AGGAGGG, FAM-duplex, CGCGCGCGTTTTCGCGCGCG) were diluted from stock to the required concentration (10μM) in 10 mM Tris-HCl buffer, pH 7.4, in the presence of 100 mM KCl, and then annealed by heating at 95 ℃ for 5 min, gradually cooled to room temperature, and incubated at 4 °C overnight. The ligands concentration was varied from 0 to 200 μM for tested the K_D of duplex DNA. A 16-point dilution series was prepared for each DNA. After incubation, the samples were loaded into MST standard-treated glass capillaries. The binding affinity study was investigated on the microscale thermophoresis instrument (NanoTemper Tchnologies GmbH, Munich, Germany). The value of K_d was calculated by NT ANALYSIS SOFTWARE provided by NanoTemper Technologies GmbH.

5. Conclusions

The chemical synthesis of one derivative of berberine and seven derivatives of palmatine showed how the further presence of side chains on the base structure of these compounds is important to improve their interaction with G-quadruplex and its stability. Some attempts in this sense have been already made in the past but there's still a lot to do since this is only the beginning of this research line. Anyway, this review clearly demonstrated that this works. The perspective for the future are unlimited with the hope to finally find the perfect compound with strong anticancer activity.

Author Contributions

All the authors contributed equally to every part of the work.

Conflicts of Interest

The authors declare no potential conflict of interests

References

1. Huppert, J.L. Four-stranded nucleic acids: structure, function and targeting of G-quadruplexes. *Chem. Soc. Rev.* **2008**, *37(7)*, 1375-1384.

2. Sen, D.; Gilbert, W. A sodium-potassium switch in the formation of four-stranded G4-DNA. *Nature* **1990**, *344(6265)*, 410-414.

3. Parkinson, G.N.; Lee, M.P.; Neidle, S. Crystal structure of parallel quadruplexes from human telomeric DNA. *Nature* **2002**, *417(6891)*, 876-880.

4. Cogoi, S.; Xodo, L.E. G-quadruplex formation within the promoter of the KRAS proto-oncogene and its effect on transcription. *Nucleic Acids Res.* **2006**, *34(9)*, 2536-2549.

5. Dexheimer, T.S.; Sun, D.; Hurley, L.H. Deconvoluting the structural and drug-recognition complexity of the G-quadruplex-forming region upstream of the bcl-2 P1 promoter. *J. Am. Chem. Soc.* **2006**, *128(16)*, 5404-5415.

6. Fernando, H.; Reszka, A.P.; Huppert, J.; Ladame, S.; Rankin, S.; Venkitaraman, A.R.; Neidle, S.; Balasubramanian, S. A conserved quadruplex motif located in a transcription activation site of the human c-kit oncogene. *Biochem.* **2006**, *45(25)*, 7854-7860.

7. Arora, A.; Dutkiewicz, M.; Scaria, V.; Hariharan, M.; Maiti, S.; Kurreck, J. Inhibition of translation in living eukaryotic cells by an RNA G-quadruplex motif. *RNA* **2008**, *14(7)*, 1290-1296.

8. Wang, Q.; Liu, J.Q.; Chen, Z.; Zheng, K.W.; Chen, C.Y.; Hao, Y.H.; Tan, Z. G-quadruplex formation at the 3' end of telomere DNA inhibits its extension by telomerase, polymerase and unwinding by helicase. *Nucleic Acids Res.* **2001**, *39*, 6229-6237.

9. Maizels, N. Dynamic roles for G4 DNA in the biology of eukaryotic cells. *Nat. Struct. Mol. Biol.* **2006**, *13(12)*, 1055-1059.

10. Qin, Y.; Hurley L.H. Structures, folding patterns, and functions of intramolecular DNA G-quadruplexes found in eukaryotic promoter regions. *Biochimie* **2008**, *90(8)*, 1149-1171.

11. Kittakoop, P.; Mahidol, C.; Ruchirawat, S. Alkaloids as important scaffolds in therapeutic drugs for the treatments of cancer, tuberculosis, and smoking cessation. *Curr. Top. Med. Chem.* **2014**, *14(2)*, 239-252.

12. Russo, P.; Frustaci, A.; Del Bufalo, A.; Fini, M.; Cesario, A. Multitarget drugs of plants origin acting on Alzheimer's disease. *Curr. Med. Chem.* **2013**, *20(13)*, 1686-1693.

13. Raymond Sinatra, S.; Jahr, J.S.; Watkins-Pitchford, J.M. *The Essence of Analgesia and Analgesics*; Cambridge University Press: Cambridge, UK, 2010; pp. 82-90; ISBN 1139491989.

14. Cushnie, T.P.; Cushnie, B.; Lamb, A.J. Alkaloids: An overview of their antibacterial, antibiotic-enhancing and antivirulence activities. *Int. J. Antimicrob. Agents.* **2014**, *44(5)*, 377-386.

15. Qiu, S.; Sun, H.; Zhang, A.H.; Xu, H.Y.; Yan, G.L.; Han, Y.; Wang, X.J. Natural alkaloids: basic aspects, biological roles, and future perspectives. *Chin. J. Nat. Med.* **2014**, *12(6)*, 401-406.

16. Naasani, I.; Seimiya, H.; Yamori, T.; Tsuruo, T. FJ5002: a potent telomerase inhibitor identified by exploiting the disease-oriented screening program with COMPARE analysis. *Cancer Res*. **1999**, *59(16)*, 4004-4011.

17. Ji, X.; Sun, H.; Zhou, H.; Xiang, J.; Tang, Y.; Zhao, C. The interaction of telomeric DNA and C-myc22 G-quadruplex with 11 natural alkaloids. *Nucleic Acid Ther.* **2012**, *22(2)*, 127-136.

18. Imanshahidi, M.; Hosseinzadeh, H. Pharmacological and therapeutic effects of *Berberis vulgaris* and its active constituent, berberine. *Phytother. Res.* **2008**, *22*, 999-1012.

19. Yan, D.; Jin, C.; Xia, X.; Dong, X. Antimicrobial properties of berberines alkaloids in *Coptis chinensis* Franch by microcalorimetry. *J. Biochem. Biophys. Methods*. **2008**, *70(6)*, 845-849.

20. Schmeller, T.; Latz-Bróning, B.; Wink, M. Biochemical activities of berberine, palmatine and sanguinarine mediating chemical defence against microorganisms and herbivores. *Phytochem.* **1997**, *44(2)*, 257-266.

21. Slaninová, I.; Táborská, E.; Bochoráková, H.; Slanina, J. Interaction of benzo[c]phenanthridine and protoberberine alkaloids with animal and yeast cells. *Cell. Biol. Toxicol.* **2001**, *17*, 51-63.

22. Zhang, W.J.; Ou, T.M.; Lu, Y.J.; Huang, Y.Y.; Wu, W.B.; Huang, Z.S.; Zhou, J.L.; Wong, K.Y.; Gu, L.Q. 9-Substituted berberine derivatives as G-quadruplex stabilizing ligands in telomeric DNA. *Bioorg. Med. Chem.* **2007**, *15(16)*, 5493-5501.

23. Franceschin, M.; Rossetti, L.; D'Ambrosio, A.; Schirripa, S.; Bianco, A.; Ortaggi, G.; Savino, M.; Schultes, C.; Neidle, S. Natural and synthetic G-quadruplex interactive berberine derivatives. *Bioorg. Med. Chem.* **2006**, *16(6)*, 1707-1711.

24. Bhadra, K.; Kumar, G.S. Interaction of berberine, palmatine, coralyne, and sanguinarine to quadruplex DNA: A comparative spectroscopic and calorimetric study. *Biochim. Biophys. Acta (BBA) - General Subjects.* **2011**, *1810(4)*, 485-496.

25. Zhou, Q.; Li, L.; Xiang, J.; Tang, Y.; Zhang, H.; Yang, S.; Li, Q.; Yang, Q.; Xu, Q. Screening potential antitumor agents from natural plant extracts by G-Quadruplex recognition and NMR methods. *Angew. Chem. Int. Ed.* **2008**, *47*, 5590-5592.

26. Jana, J.; Kar, R.K.; Ghosh, A.; Biswas, A.; Ghosh, S.; Bhunia, A.; Chatterjee, S. Human cathelicidin peptide LL37 binds telomeric G-quadruplex. **Mol Biosyst.** *2013*, **9(7)**, 1833-1836.

27. Huang, L.; Shi, A,; He, F.; Li, X..Synthesis, biological evaluation, and molecular modeling of berberine derivatives as potent acetylcholinesterase inhibitors. *Bioorg. Med. Chem.* **2010**, *18(3)*, 1244-1251.

28. Zhou, J.L.; Lu, Y.J.; Ou, T.M.; Zhou, J.M.; Huang, Z.S.; Zhu, X.F.; Du, C.J.; Bu, X.Z.; Ma, L.; Gu, L.Q.; Li, Y.M.; Chan, A.S. Synthesis and evaluation of quindoline derivatives as G-quadruplex inducing and stabilizing ligands and potential inhibitors of telomerase. *J. Med. Chem.* **2005**, *48(23)*, 7315-7321.

29. Rossetti, L.; Franceschin, M.; Bianco, A.; Ortaggi, G.; Savino, M. Perylene diimides with different side chains are selective in inducing different G-quadruplex DNA structures and in inhibiting telomerase. *Bioorg. Med. Chem. Lett.* **2002**, *12*, 2527-2533.

30. Rossetti, L.; Franceschin, M.; Schirripa, S.; Bianco, A.; Ortaggi, G.; Savino, M. Selective interactions of perylene derivatives having different side chains with inter- and intramolecular G-quadruplex DNA structures. A correlation with telomerase inhibition. *Bioorg. Med. Chem. Lett.* **2005**, *15*, 413-420

31. Latimer, L.J.; Payton, N.; Forsyth, G.; Lee, J.S. The binding of analogues of coralyne and related heterocyclics to DNA triplexes. *Biochem. Cell Biol.* **1995**, *73(1-2)*, 11-18.

32. Husby, J.; Todd, A.K.; Platts, J.A.; Neidle, S. Small-molecule G-quadruplex interactions: Systematic exploration of conformational space using multiple molecular dynamics. *Biopolymers*. **2013**, *99*, 989-1005.

33. Fedoroff, O.Y.; Salazar, M.; Han, H.; Chemeris, V.V.; Kerwin, S.M.; Hurley, L.H. NMR-Based model of a telomerase-inhibiting compound bound to G-quadruplex DNA. *Biochemistry*. **1998**, *37*, 12367-12374.

34. Peng, D.; Tan, J.H.; Chen, S.B.; Ou, T.M.; Gu, L.Q.; Huang, Z.S. Bisaryldiketene derivatives: a new class of selective ligands for c-myc G-quadruplex DNA. *Bioorg. Med. Chem.* **2010**, *18(23)*, 8235-8242.

35. De Cian, A.; Guittat, L.; Kaiser, M.; Saccà, B.; Amrane, S.; Bourdoncle, A.; Alberti, P.; Teulade-Fichou, M.P.; Lacroix, L.; Mergny, J.L. Fluorescence-based melting assays for studying quadruplex ligands. *Methods*. **2007**, *42(2)*, 183-195.

36. Mao, Y.; Yu, L.; Yang, R.; Qu, L.B.; Harrington Pde, B. A novel method for the study of molecular interaction by using microscale thermophoresis. *Talanta*. **2015**, *132*, 894-901.

37. Jerabek-Willemsen, M.; Wienken, C.J.; Braun, D.; Baaske, P.; Duhr, S. Molecular interaction studies using microscale thermophoresis. *Assay Drug Dev. Technol.* **2011**, *9(4)*, 342-353.

38. Gan, Y.; Lu, J.; Johnson, A.; Wientjes, M.G.; Schuller, D.E.; Au, J.L. A quantitative assay of telomerase activity. *Pharm. Res.* **2001**, *18(4)*, 488-493.

39. Nechepurenko, I.V.; Komarova, N.I.; Vasil'ev, V.G.; Salakhutdinov, N.F. Synthesis of berberine bromide analogs containing tertiary amides of acetic acid in the 9-O-position. *Chem. Nat. Compd*. **2013**, *48(6)*, 1047-1053.

40. Rachwal, P.A.; Fox, K.R. Quadruplex melting. *Methods*. **2007**, *43(4)*, 291-301.

Preprints (www.preprints.org) | NOT PEER-REVIEWED | Posted: 14 May 2018 doi:10.20944/preprints201805.0189.v1

Peer-reviewed version available at Molecules 2018, 23, 1423; doi:10.3390/molecules23061423

Figures, Schemes and Tables

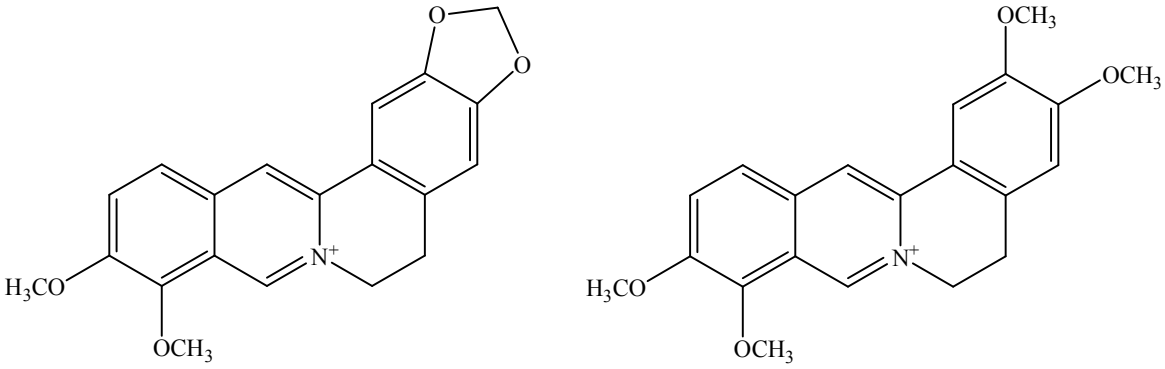

Figure 1: Structures of berberine and palmatine

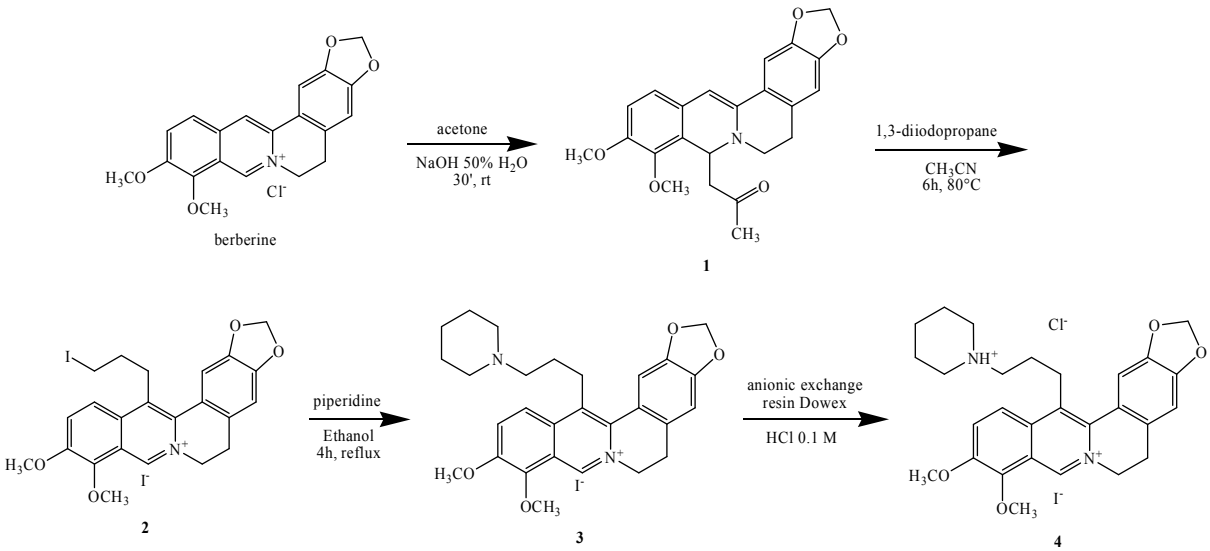

Scheme 1: Synthesis of the berberine derivative (**4**)

Preprints (www.preprints.org) | NOT PEER-REVIEWED | Posted: 14 May 2018 doi:10.20944/preprints201805.0189.v1

Peer-reviewed version available at Molecules 2018, 23, 1423; doi:10.3390/molecules23061423

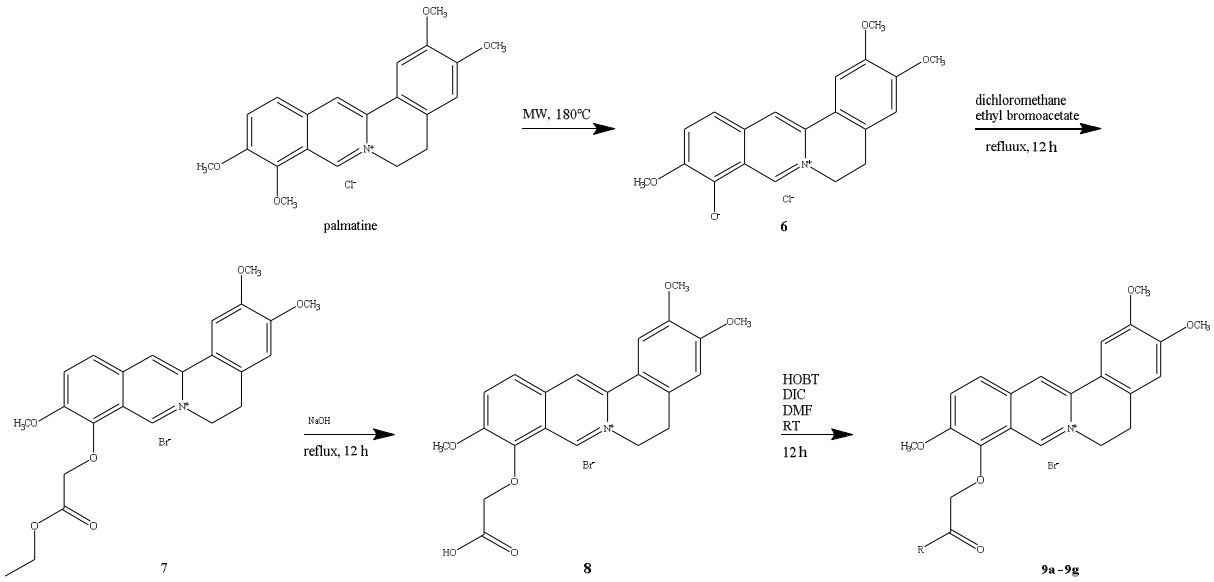

Scheme 2: Synthesis of 9-peptidyl palmatine derivatives (**9a-9g**)

Ligand	Peptide side chain
9a	K-R
9b	F-R
9c	R-R
9d	F-H-R
9e	K-F-R
9f	F-G-K
9g	F-K-R
G = Glycine; R = Arginine; K = Lysine; H = Histidine; F = Phenylalanina	

Scheme 3: Structures of the synthesized 9-peptidyl palmatine derivatives (**9a-9g**)

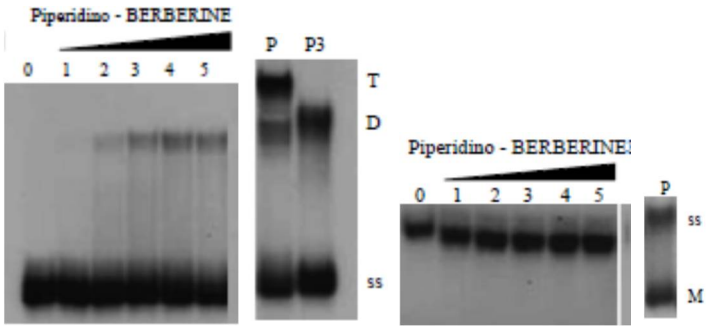

Figure 2: Results on the ability of compound (**4**) to form G-quadruplex structures

LIGAND	Bcl-2	c-Kit1	c-Myc	Htg21
9a	-8.4	-10.7	-11.1	-10.7
9b	-8.2	-10.3	-11.1	-9.3
9c	-9.0	-10.9	-10.8	-11.6
9d	-9.8	-10.8	-11.7	-11.5
9e	-9.7	-11.3	-10.9	-11.3
9f	-7.4	-10.3	-10.5	-10.5
9g	-8.9	-10.9	-11.8	-12.0
Palmatine	-2.5	-3.6	-3.09	-2.9
Berberine	-3.9	-3.3	-2.9	-2.7
Compounds were docked on four different DNA strands: Bcl-2, C-Kit1, Pu22 (c-Myc), Htg21 all in parallel conformation. Results are express in Kcal/mol.				

Table 1: Docking results for berberine, palmatine and palamtine derivatives.

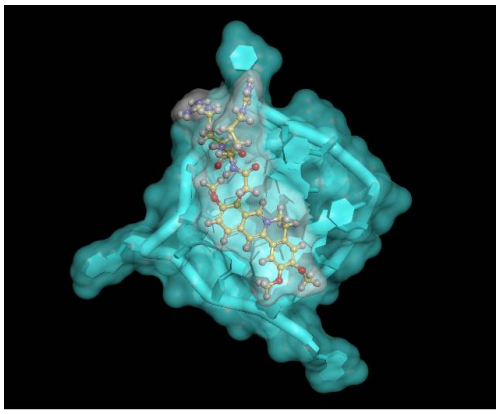

Figure 3: Interaction between DNA G-Quadruplex (C-Kit1) and 4g. Blue = DNA; Yellow = Carbon; Dark Blue = Nitrogen, Red =Oxygen

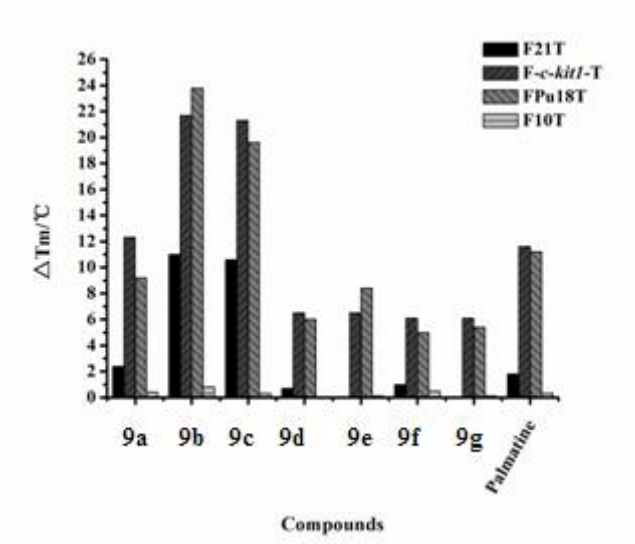

Figure 4: G-Quadruplex DNA and duplex DNA stabilization temperatures (ΔT_m) with palmatine derivatives

Ligands	R[a]	FRET (ΔT_m , ℃)			
		F21T[b]	Fc-*kit*1T[b]	FPu18T[b]	F10T[b]
9a	KR-NH_2	2.4 ± 0.8	12.3 ± 0.2	9.2 ± 0.5	0.4 ± 0.9
9b	FR-NH_2	11.0 ± 0.1	21.7 ± 0.8	23.8 ± 0.6	0.8 ± 0.4
9c	RR-NH_2	10.6 ± 0.2	21.3 ± 0.5	19.6 ± 0.9	0.3 ± 0.6
9d	FHR-NH_2	0.7 ± 0.7	6.5 ± 0.2	6.0 ± 1.0	0.0 ± 1.0
9e	KFR-NH_2	0.0 ± 1.2	6.5± 0.4	8.4 ± 0.3	0.1 ± 1.0
9f	FGK-NH_2	1.0 ± 0.6	6.1 ± 0.9	5.0 ±1.0	0.5 ± 0.1
9g	FKR-NH_2	0.0 ±1.0	6.1 ± 0.4	5.4 ± 0.2	0.1 ± 1.0
palmatine	--	1.8 ± 0.2	11.6 ± 0.2	11.2 ± 0.1	0.3 ± 0.3

[a] R is the peptidyl sequences of these conjugates side chains, starting from the terminal of scaffold. R, G, F, H, and K are abbreviations of Arginine, Glycine, Phenylalanine, Histidine, and Lysine, respectively. [b] $\Delta T_m = T_m$ (DNA + ligand) - T_m (DNA). ΔT_m values of 0.2μM F21T , Fc-*kit*1T, FPu18T or F10T incubated with 1.0 μM compound in the presence of 60 mM KCl.

Table 2. G-Quadruplex DNA and duplex DNA stabilization temperatures (ΔT_m) obtained from FRET melting assay

Preprints (www.preprints.org) | NOT PEER-REVIEWED | Posted: 14 May 2018 doi:10.20944/preprints201805.0189.v1

Peer-reviewed version available at Molecules 2018, 23, 1423; doi:10.3390/molecules23061423

Compounds	R[a]	*c-kit1* (K_d, μM)	duplex (K_d, μM)	$K_d^{duplex}/K_d^{c\text{-}kit1}$
9a	KR	2.65 ± 0.33	23.60 ± 1.07	8.9
9b	FR	1.41 ± 0.09	10.70 ± 1.30	7.6
9c	RR	1.47 ± 0.12	20.40 ± 0.96	13.9
9d	FHR	9.68 ± 0.57	40.70 ± 5.87	4.2
9e	KFR	8.00 ± 0.89	16.80± 1.38	2.1
9f	FGK	11.10 ± 0.51	40.70 ± 1.62	3.7
9g	FKR	6.60 ±0.472	45.50 ±4.57	6.9
palmatine	--	3.25 ± 0.32	5.08 ± 0.34	1.6

[a] R is the peptidyl sequences of these conjugates side chains, starting from the terminal of scaffold. R, G, F, H, and K are abbreviations of Arginine, Glycine, Phenylalanine, Histidine, and Lysine, respectively.

Table 3: Kinetic constants of palmatine derivatives with *c-kit1* G-quadruplex and duplex DNA by MST assay

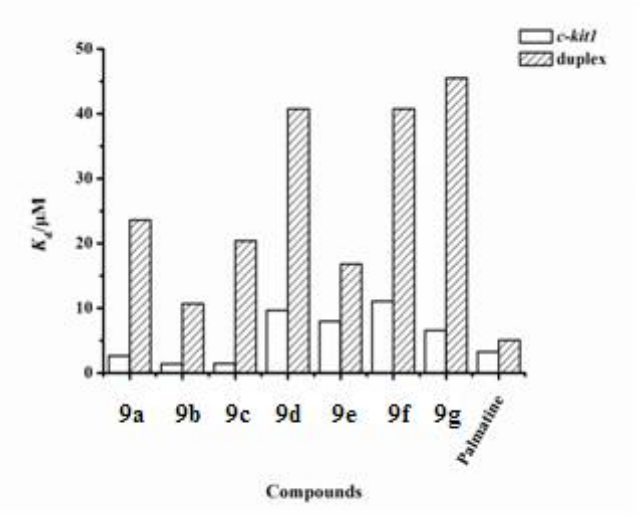

Figure 5: Graphic of the dissociation constants of palmatine derivatives with *c-kit1* G-quadruplex and duplex DNA by MST

Ligands	R[a]	Bond Energy (kcal/mol)		
		Htg21	*c-kit1*	*c-myc*
9a	KR-NH_2	-10.7	-10.7	-11.8
9b	FR-NH_2	-9.9	-10.3	-11.1
9c	RR-NH_2	-11.3	-10.8	-10.7
9d	FHR-NH_2	-11.6	-10.8	-11.3
9e	KFR-NH_2	-11.3	-11.3	-10.9
9f	FGK-NH_2	-10.5	-10.3	-10.5
9g	FKR-NH_2	-12.0	-10.9	-11.8
palmatine	--	-2.9	-3.5	-3.1

[a] R is the peptidyl sequences of these conjugates side chains, starting from the terminal of scaffold. R, G, F, H, and K are abbreviations of Arginine, Glycine, Phenylalanine, Histidine, and Lysine, respectively.

Table 4: Energetic values of the bond between palmatine derivatives with *c-kit1* G-quadruplex and duplex DNA by MST assay

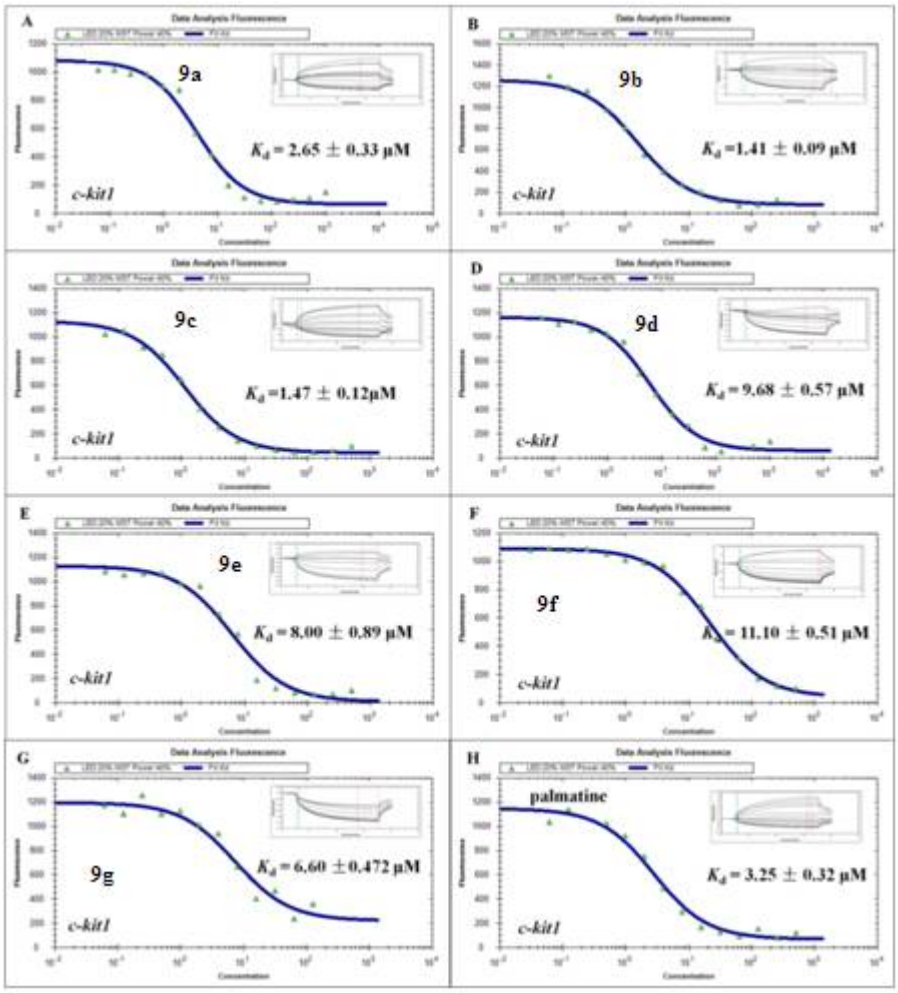

Figure 6: The binding affinity study of palmatine derivates with *c-kit1* G-quadruplex DNA by MST

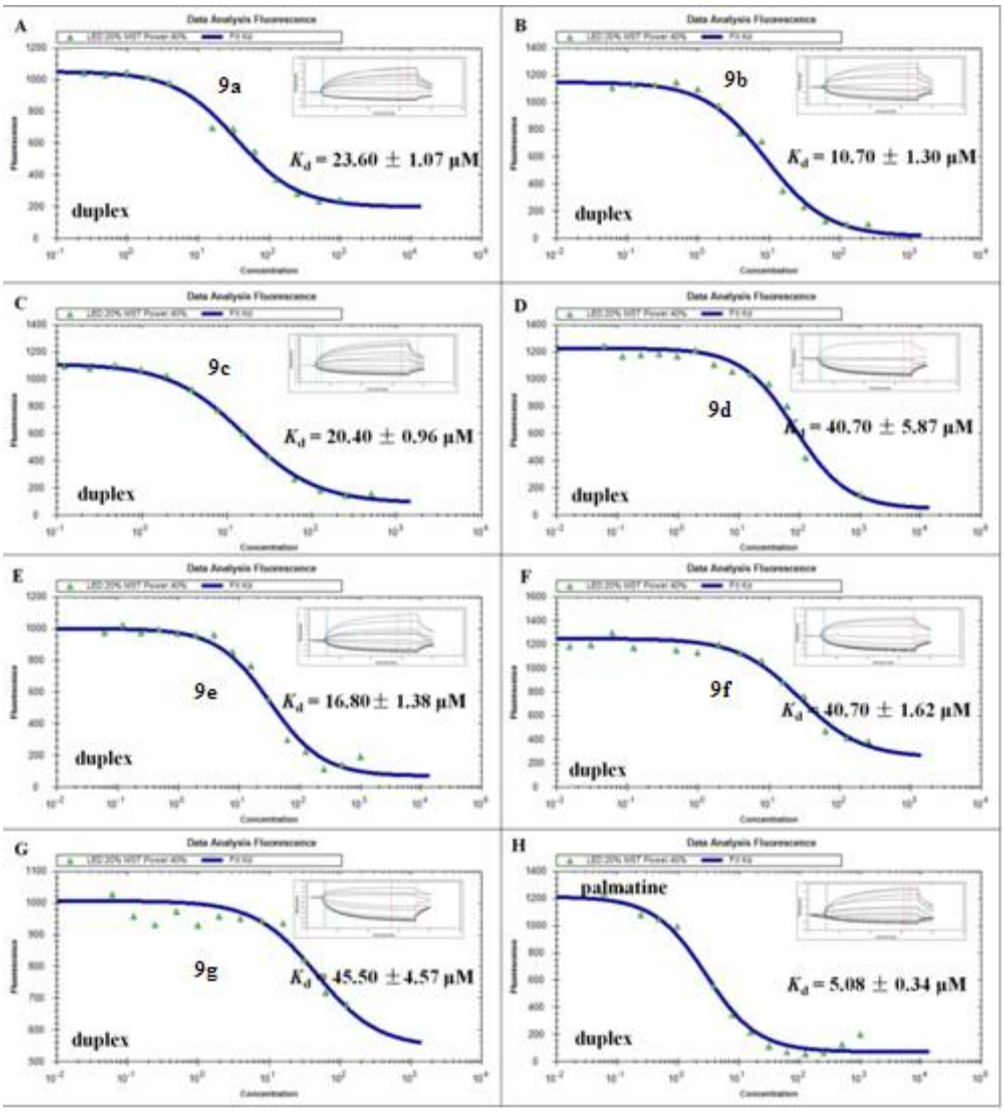

Figure 7: The binding affinity study of palmatine derivates with duplex DNA by MST

Preprints (www.preprints.org) | NOT PEER-REVIEWED | Posted: 14 May 2018 doi:10.20944/preprints201805.0189.v1

Peer-reviewed version available at Molecules 2018, 23, 1423; doi:10.3390/molecules23061423

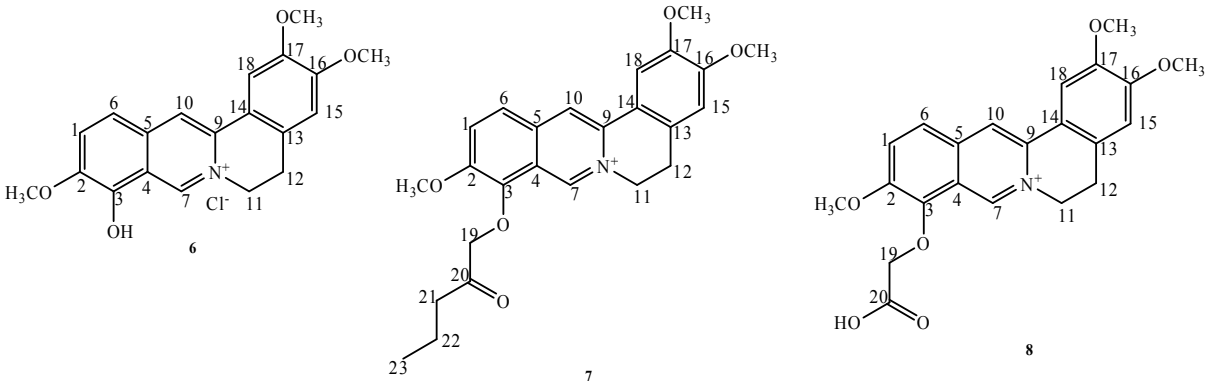

Figure 8: Structures of compounds (**6-8**)

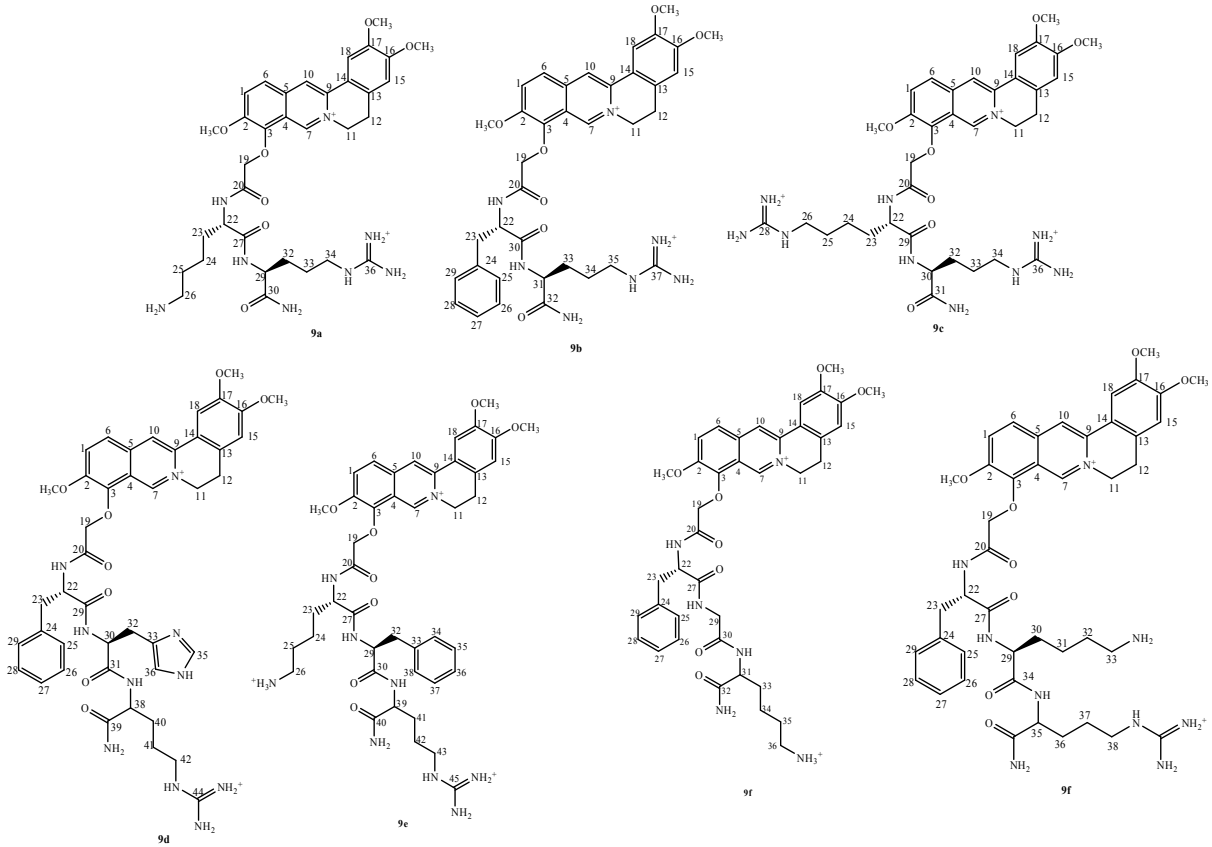

Figure 9: Structures of compounds (**9a-9g**)

G-quadruplex name	PDB ID
c-*myc* parallel	1XAV
c-*kit* parallel	2O3H
Bcl-2 parallel	2F8U
Htg21 parallel	2KZE

Table 5: G-quadruplex structures used in molecular docking